A sensitivity analysis of numerical predictions for beryllium erosion and migration in ITER

J. Romazanov*[a], S. Brezinsek[a], R. A. Pitts[b], A. Kirschner[a], A. Eksaeva[a], D. Borodin[a], E. Veshchev[b], V. S. Neverov[c], A. B. Kukushkin[c], A. G. Alekseev[c], and Ch. Linsmeier[a]

[a]Forschungszentrum Jülich GmbH, Institut für Energie- und Klimaforschung – Plasmaphysik, Partner of the Trilateral Euregio Cluster (TEC), 52425 Jülich, Germany
[b]ITER Organization, Route de Vinon-sur-Verdon, CS 90 046, 13067, St. Paul Lez Durance Cedex, France
[c]National Research Centre 'Kurchatov Institute', Moscow 123182, Russia

September 15, 2020

Abstract

The present study addresses the uncertainties that affect the recently performed predictions of beryllium (Be) erosion and migration in ITER using the Monte-Carlo code ERO2.0. The focus of the study is a D-T baseline discharge with fusion power gain $Q = 10$, scrape-off layer (SOL) input power $P_{\mathrm{SOL}} = 100\,\mathrm{MW}$, toroidal plasma current $I_p = 15\,\mathrm{MA}$, and central toroidal field $B_t = 5.3\,\mathrm{T}$. The parameter studies used to investigate uncertainties include variations of the radial extrapolation of plasma parameters in the far-SOL (scan A), the assumptions on impact angle distributions (scan B) and the anomalous transport of eroded Be (scan C). Variations by factors ~ 3, ~ 18 and ~ 2 for scans A, B and C, respectively, are found.

keywords: *beryllium, erosion, migration, ERO2.0, ITER*

1 Introduction

Steady-state erosion of the ITER main chamber first wall (FW) beryllium (Be) armour is expected to affect several processes important for the reactor duty cycle. Among these are armour degradation and lifetime, dust formation, and release of Be impurities potentially

*JARA-HPC, Jülich Supercomputing Centre, Forschungszentrum Jülich GmbH, Jülich 52425, Germany

leading to dilution of the core plasma, enhanced sputtering of the W divertor, and tritium retention due to co-deposition. Reliable numerical estimations of the Be erosion and migration are necessary to quantify these effects, but also to support the development of ITER diagnostics, designed for monitoring the Be primary source, by providing synthetic signals.

A first application of the Monte-Carlo code ERO2.0 for this task was reported recently [1], followed by an extended study for different ITER plasma scenarios [2]. The code simulates the steady-state Be erosion flux resulting from ion and charge-exchange neutral (CXN) bombardment of the entire ITER FW, taking into account the subsequent kinetic transport of eroded Be impurities. The latter are represented by so-called test particles, which are used in a Monte-Carlo formalism to solve the Fokker-Planck equation in the trace impurity approximation [3]. The three-dimensional (3D) shaping of the FW panels is taken into account, which is important due to magnetic shadowing effects affecting the flux distribution and the strong dependence of sputtering yields on the particle impact angle.

This contribution addresses the sensitivity of the ERO2.0 predictions regarding (1) the extrapolation of plasma parameters near the FW panel surfaces, (2) the assumptions on particle impact angle distributions, and (3) the anomalous transport of eroded Be released into the SOL plasma. The main results of the modelling studies are summarized in Table 1.

2 Parameter studies

2.1 Reference modelling assumptions

All simulations in this study are based on the baseline H-mode D-T burning plasma scenario with toroidal plasma current $I_p = 15\,\mathrm{MA}$, central toroidal field $B_t = 5.3\,\mathrm{T}$, fusion power gain $Q = 10$, and input power $P_{\mathrm{SOL}} = 100\,\mathrm{MW}$ into the scrape-off layer (SOL) [4] ("reference case"). This scenario is labelled "case #1" in the wider study reported in [2], where also other plasma scenarios are considered. Note that similar parameters were also used in the initial ERO2.0 study of ITER main chamber Be erosion/migration in [1], which, however, assumed a very high imposed parallel SOL flow ($M = 0.5$). Here in contrast, only "source-sink" driven flows extracted from SOLPS 4.3 [5] simulations are considered.

SOLPS-4.3 coupled to OEDGE [6] simulations provide the input plasma background (PBG) to ERO2.0, i.e. the spatial distribution of plasma parameters in the boundary region. OEDGE extends the grid to the wall using a combination of onion skin modelling (OSM) and the kinetic neutral transport code EIRENE [7]. In addition, OEDGE considers the so-called ITER Heat and Nuclear Load Specifications (HNLS) [8] as a constraint for the far-SOL plasma. The OEDGE extended grid and the underlying SOLPS-4.3 solution regions are shown in Figure 1(a), which also shows the magnetic configuration and the locations of the 18 FW panels in the ITER poloidal cross-section. Note that both SOLPS-4.3 and OSM are 2D codes, so that the resulting 2D PBG cannot account for the 3D FW shaping and is thus assumed to extend only to the innermost radial locations of FW panels in the poloidal cross-section. This necessitates the extrapolation of plasma profiles in the radial outward direction, as discussed in detail in the next section. In addition, numerical tracing of magnetic field lines is used to define plasma-wetted and shadowed areas (the latter are excluded from erosion by ions) on the 3D surface, as shown in Figure 1(b). The shadowing

model is described in detail in [1].

The simulations with the massively-parallelised ERO2.0 code were performed on the JURECA supercomputer [9]. The requirement for supercomputing resources comes from the large number of Be test particles (10^6 for the calculations reported here) that are necessary in production runs to achieve sufficiently reproducible results with acceptable Monte-Carlo noise. As a simplification, the D-T plasma is described as a pure D plasma (as is the case, in fact, for the SOLPS PBG simulations). Furthermore, Be is considered to be the only impurity, though the PBG considers neon seeding for power dissipation in the divertor.

The Be sputtering yields used to calculate the erosion are discussed in more detail in [2]. Note that chemically assisted physical sputtering with release of BeD molecules [10] is neglected here for simplicity, so that all erosion is assumed to be in the form of Be atoms.

In the following, the individual parameter scans will be presented. Note that during each scan, all other parameters are kept as in the reference case.

2.2 Parameter scan A: Influence of far-SOL plasma conditions

Some modifications of the OEDGE data are required due to the 3D shaping of the FW panels considered in the ERO2.0 modelling. Despite the extended grid in the PBG, the shaping leads to a small gap Δr_{gap} between the outer OEDGE grid and the FW surface cells. The gap size is mostly about 0–3 cm in the plasma-wetted areas, as shown in Figure 1(b). To be consistent with the (conservative) assumption in the ITER HNLS, the default approach in ERO2.0 is to extend the radial plasma profiles in the gap region using constant ("flat") extrapolation, as shown in the outer mid-plane (OMP) profiles in Figure 2. However, a more realistic expectation would be that the profiles decay radially, resulting in much lower ion impact fluxes and energies and hence Be erosion.

For simplicity and to maintain particle balance with OEDGE, the ion impact flux decay was not considered here and the decay was applied solely to the T_{e} and T_{i} profiles. In the frame of "parameter scan A" described in this section, different decay lengths, $\lambda = 0.1$ cm, 1.0 cm and 10.0 cm, were initially considered for the extrapolation of T_{e} and T_{i} to the FW as depicted in Figure 2.

The above values of λ are selected on the basis of typical experimental values from various plasma devices, which are scattered within the range of $\lambda \sim 0.1$–10 cm.[1] Furthermore, numerical estimates were performed using the connection lengths L calculated by ERO2.0 field line tracing, combined with either diffusive or convective models for $\lambda(L)$ and the associated perpendicular transport to the wall. The considered range of input parameters (e.g. $D = 0.1$–$10.0\,\mathrm{m}^2/\mathrm{s}$ for the diffusive model) again led to $\lambda \sim 0.1$–10 cm, so that the parametric approach chosen here seems reasonable.

Preliminary simulations have shown that there is no appreciable difference in the Be erosion pattern and magnitude between the $\lambda = 10.0$ cm and $\lambda = \infty$ cases. The former is therefore not further considered here in the following.

Figure 3 shows the Be erosion rate integrated over the entire ITER FW. The contribution to the erosion by D^0 impact is by definition constant because ERO2.0 imports D^0 fluxes and energies directly from OEDGE, which are therefore not affected by the plasma parameter

[1] See Figures 21.1, 21.2, 21.3, 21.8, 21.9 and 23.2 in [11].

extrapolation. In contrast, the contribution by D^+ impact is decreased for smaller λ because the D^+ impact energy is proportional to T_e (determining the sheath potential) and T_i (determining the ion energy at the sheath entrance). Likewise, the contribution due to Be^+ impact is decreased for smaller λ both because fewer Be particles are eroded in the first place, and due to a decrease in their impact energy by the lower sheath potential.

In the $\lambda = 1\,\mathrm{cm}$ case, the total erosion is decreased by 50 % compared to the reference $\lambda = \infty$ case. For $\lambda = 0.1\,\mathrm{cm}$, the decrease is 65 %. It is expected that further reduction below 0.1 cm would only lead to a gradual decrease in erosion (saturation effect), because some regions exist with a very small gap $\Delta r \ll 0.1\,\mathrm{cm}$ or even with no gap, which are not subject to extrapolation.

It should be noted that $\lambda = 0.1\,\mathrm{cm}$ is already at the lower end of the experimental values found in literature and the numerical estimations using a diffusive or convective model. Values of (density or temperature) decay lengths $\lambda \sim 1\,\mathrm{cm}$ or higher seem more probable. Thus, the result of this scan in the far-SOL plasma parameter extrapolation may be summarized by noting that the conservative assumption of $\lambda = \infty$ likely leads to an overestimation of the Be erosion by up to a factor ∼2. However, it must also be stressed that in the present approach, λ affects only the small extrapolation region shown in Figure 2. Applying an exponential decay in the OEDGE extended grid region (pink shaded zone in Figure 2), instead of the currently used flat curve fixed for consistency with the ITER HNLS assumptions, will lead to a more significant reduction of the predicted erosion.

2.3 Parameter scan B: Influence of particle impact angles

ERO2.0 requires assumptions on the impact velocity distributions of background D ions and neutrals to calculate the erosion, since these distributions are not contained in the input PBG. The following assumptions were used as default (reference case): (a) for D ions, the impact energy and angular distributions are obtained for each cell using a sheath tracing module built into ERO2.0, which is based on the approach described in more detail in [12]; (b) for D neutrals, the energy is set to the mean energy (provided by the PBGs) and the angle is set to the magnetic inclination angle θ_B. The plasma-wetted areas of the FW are associated with oblique magnetic inclination angles of $\theta_B > 80°$. Thus, with the above assumptions, neutrals have the same oblique impact angles $\theta = \theta_B$, whereas ions have distributions at about $\langle\theta\rangle \approx 70°$ and $\mathrm{FWHM} \approx 20°$ as shown in Figure 4.

The assumption of $\theta = \theta_B$ for the neutrals is a strong simplification. Moreover, the Be FW is assumed in the modelling as a perfectly smooth surface. However, in reality the surface of FW components in ITER can be expected to exhibit a microscale roughness [13], which will, along with other factors, affect the impact angle distributions. The same is true for the castellation of the panels, which was neglected here.

The Be sputtering yields are very sensitive to the impact angle, with a maximum at about $\theta \approx 80°$ [2]. It is therefore important to investigate the dependence of the overall erosion on the impact angle, considering the entire possible range $\theta = 0$–$90°$. In "parameter scan B", the particle impact assumptions are changed in the following way: for both ions and neutrals, the impact angle is set to a constant value θ_0 for all surface cells, regardless of the local geometry and plasma conditions. The value of θ_0 is subject to a parameter scan, with $\theta_0 = 0°, 60°, 75°, 80°$ and $85°$ for each simulation, respectively. Since the sheath tracing

module was disabled in this scan, the ion energy distribution was simplified to the well-known analytic expression $E = 2T_i + q|V_{\mathrm{sheath}}|$, where the first term is the thermal energy at the sheath entrance, and the second term is the energy gain due to the sheath acceleration [11, p. 629].

Figure 5 shows the total, surface-integrated FW Be erosion plotted over the impact angle. In addition, the individual contributions of D^+, D^0 and Be^{Z+} impact are shown. Note that although the Be impact velocity distributions are unaffected by the variations of the D impact assumptions performed in this section (since Be velocities are calculated self-consistently from the test particle trajectories), the erosion by Be^{Z+} impact is nevertheless affected due to the change of the Be concentration in the plasma.

Due to an interplay of the angular dependencies of the Be sputtering yields for D and self-impact, the maximum of the total erosion is reached at about $\theta_0 = 80$–$85°$. The maximum value of $\Gamma_{\mathrm{Be}}^{\mathrm{ero}}(\theta_0 = 80°) = 2.35 \times 10^{23}\,\mathrm{Be/s}$ is about 53 % higher than the reference case value of $1.53 \times 10^{23}\,\mathrm{Be/s}$ achieved with the broader impact angle distributions. On the other hand, the minimum value with $\Gamma_{\mathrm{Be}}^{\mathrm{ero}}(\theta_0 = 0°) = 1.28 \times 10^{22}\,\mathrm{Be/s}$ is roughly 12x lower than the reference case value. One can estimate by linear interpolation that an erosion similar to the reference case can be achieved with a constant impact angle $\theta_0 \approx 70°$.

We can summarize that the reference case erosion of $1.53 \times 10^{23}\,\mathrm{Be/s}$ is in the upper middle part of the possible range 0.13–$2.35 \times 10^{23}\,\mathrm{Be/s}$ that can be achieved by varying the impact angle between 0–90°. However, an assessment, validation or improvement of the impact angle distributions resulting from the reference assumptions would require knowledge of the surface roughness. In the case of the D neutrals, further insight could be gained in the future by using angular and energy distributions from EIRENE post-processing of the plasma backgrounds, combined with parameter studies using different types of roughness.

3 Parameter scan C: Influence of anomalous transport

ERO2.0 uses a freely defined diffusion coefficient $D_\perp$ to account for anomalous cross-field transport of the Be test particles. The reference ERO2.0 case uses $D_\perp = 1\,\mathrm{m^2/s}$, which is a typical empirically found value[2], and is assumed here to be constant in the entire simulation domain. The choice of $D_\perp$ affects the transport of Be and its redeposition on the FW (thus net erosion), and also the Be self-sputtering. Therefore, "parameter scan C" includes simulations with two different values for $D_\perp$ for Be transport: (1) a lower diffusion coefficient $D_\perp = 0.3\,\mathrm{m^2/s}$ corresponding to the value used for D plasma transport in the OEDGE simulations, and (2) a higher diffusion coefficient $D_\perp = 10\,\mathrm{m^2/s}$.

Figure 6 shows the total Be erosion for $D_\perp = 0.3\,\mathrm{m^2/s}$ and $D_\perp = 10\,\mathrm{m^2/s}$ along with the reference case $D_\perp = 1.0\,\mathrm{m^2/s}$. For $D_\perp = 0.3\,\mathrm{m^2/s}$, the total erosion is 28 % higher than in the reference case. For $D_\perp = 10\,\mathrm{m^2/s}$ it is 37 % lower. Since $D_\perp$ affects only the Be transport in the ERO2.0 simulations, this change in erosion is entirely due to the self-sputtering contribution. As seen in Figure 6 and Table 1, in the reference case Be self-impact contributes 56.2 % of the total erosion, while it is 65.8 % and 31.1 % in the $D_\perp = 0.3$ and $10.0\,\mathrm{m^2/s}$ cases, respectively.

[2] See [11], pp. 15, 158, 283.

As seen in Table 1, increasing $D_\perp$ leads to a slightly increased Be redeposition flux on the FW (which can be explained by shorter migration paths due to higher probability of returning to the wall by cross-field transport). However, the changes in the Be charge and impact velocity distributions eventually lead to a decrease of the self-sputtering that far outweighs the increased flux. The Be charge and impact velocity distributions, accumulated over the entire FW, are shown in Figure 7. Increasing $D_\perp$ leads to a shift in the direction of lower charge states, impact energies and angles, and thus reduced self-sputtering.

The observed decrease in charge state and impact energy can be attributed to the shorter migration paths of Be at higher $D_\perp$. In turn, the lower charge state and energy at the sheath entrance affects the final part of the Be trajectories in the sheath which determine the impact angle. In addition, for higher $D_\perp$, Be penetrates more frequently into shadowed areas of the FW, which (due to the toroidal shaping of the panels) is characterised by less oblique magnetic incidence, which causes a shift to lower impact angles.

In summary, the variation of the perpendicular diffusion coefficient $D_\perp$ for Be ions over a wide range 0.3–10 m^2/s leads to a variation of the total erosion in the range 0.97–1.96×10^{23} Be/s, due to the change in Be transport and Be self-sputtering. Importantly, the influence on the fractions of Be being deposited in the main chamber and divertor is negligible. The difference in self-sputtering is due to a change in the impact velocity distributions. As mentioned above, the studies here are for perfectly smooth surfaces, thus consideration of rough surfaces will affect both the re-deposition and impact angles and will change the variations observed here.

4 Conclusions

Parameter studies have been performed to investigate the uncertainties on ERO2.0 modelling of beryllium erosion and migration in ITER under burning plasma conditions. The focus was on uncertainties related to plasma parameter extrapolation (scan A), impact velocity assumptions (scan B) and Be anomalous diffusion coefficient (scan C). The resulting variations of the total Be gross erosion were 0.55–1.53×10^{23} Be/s for scan A, 0.13–2.35×10^{23} Be/s for scan B, and 0.97–1.96×10^{23} Be/s for scan C. In scan A, the reference case with $\lambda = \infty$ and 1.53×10^{23} Be/s is the most conservative with the highest erosion, while in scans B and C, the reference case is found in the midrange of the possible values.

Judging from these numbers alone, the impact angle assumptions are the largest uncertainty (factor $\sim$18 between minimum and maximum value), followed by the plasma extrapolation (factor $\sim$3) and the diffusion coefficient (factor $\sim$2). Although these error bars are very large, it must be noted that each of the scans was designed to cover a large range of values (or even the entire possible range, in the case of the impact angles). For instance, a decay length $\lambda = 0.1$ cm and an impact angle $\theta_0 = 0$ would both lead to an extreme reduction of the erosion. However, both assumptions holding simultaneously may be considered rather unrealistic. On the other hand, due to self-sputtering, the erosion depends in a non-linear way on the input parameters, which increases the overall uncertainty. Thus, a combination of moderate adjustments to input parameters could lead to a strong change of the total predicted erosion.

Further insight, and potentially a narrowing of the uncertainties, can be expected from

the following actions:

- Arguably most important is the consideration of representative surface roughnesses instead of a smooth surface, which would improve the impact angle distributions (and thus the erosion prediction) for all impinging particle species.
- Providing neutral impact energy and angular distributions from EIRENE would improve the predictions for erosion by CXN impact.
- Further reducing the gap between grid boundary and FW surface in the input plasma background, e.g. by onion skin modelling or codes like EMC3-EIRENE and the upcoming version of SOLPS-ITER with an extended-grid functionality, would render the extrapolation of plasma parameters obsolete, thus improving the erosion prediction for ion impact.
- Finally, castellation gaps were completely neglected in the present study. The majority of the erosion however is seen on enhanced heat flux (EHF) panels (e.g. 5, 8, 9), which have 12 mm square tile castellations. The castellation could potentially lead to an additional source of erosion, which could be investigated using a more precise wall geometry model that resolves the castellations.

Acknowledgements

This work has been carried out within the framework of an ITER service contract with the ID IO/CT/18/4300001791. The views and opinions expressed herein do not necessarily reflect those of the ITER Organization.

The authors gratefully acknowledge the computing time granted by the JARA-HPC Vergabegremium on the supercomputer JURECA at Forschungszentrum Jülich.

References

1. J. Romazanov *et al.*, *Contrib. to Plasma Phys.* **60**, e201900149 (2019).
2. J. Romazanov *et al.*, *"submitted to Nucl. Fusion"* (2020).
3. D. Reiser *et al.*, *J. Comput. Phys.* **377**, 219–231 (2019).
4. R. A. Pitts *et al.*, *Nucl. Mater. Energy* **20**, 100696 (2019).
5. A. S. Kukushkin *et al.*, *Fusion Eng. Des.* **86**, 2865–2873 (2011).
6. S. Lisgo *et al.*, *J. Nucl. Mater.* **438**, S580–S584 (2013).
7. D. Reiter *et al.*, *Fusion Sci. Technol.* **47**, 172–186 (2005).
8. R. A. Pitts *et al.*, *J. Nucl. Mater.* **415**, S957–S964 (2011).
9. Jülich Supercomputing Centre, *J. large-scale Res. Facil.* **4** (2018).
10. S. Brezinsek *et al.*, *Nucl. Fusion* **54**, 103001 (2014).

11. P. C. Stangeby, *The Plasma Boundary of Magnetic Fusion Devices* (IOP Publishing, Bristol and Philadelphia, 2000).

12. I. Borodkina *et al.*, *Contrib. to Plasma Phys.* **56**, 640–645 (2016).

13. A. Eksaeva *et al.*, *Nucl. Mater. Energy* **19**, 13–18 (2019).

Scan:	—	Parameter scan A		Parameter scan B					Parameter scan C	
Description:	Reference case	λ = 0.1 cm	λ = 1 cm	θ = 0°	θ = 60°	θ = 75°	θ = 80°	θ = 85°	$D_\perp$ = 0.3 m²/s	$D_\perp$ = 10 m²/s
FW gross erosion [Be/s]	1.53E+23	5.50E+22	7.57E+22	1.28E+22	1.07E+23	2.08E+23	2.35E+23	2.34E+23	1.96E+23	9.74E+22
… by D^+ impact [%]	20.7	12.7	15.4	27.6	27.8	27.4	27.4	27.4	16.1	32.5
… by D^0 impact [%]	23.1	64.5	46.8	15.9	15.7	15.8	15.9	15.8	18.1	36.4
… by Be^{Z+} impact [%]	56.2	22.9	37.8	56.5	56.5	56.8	56.7	56.7	65.8	31.1
FW net erosion [Be/s]	1.50E+22	9.37E+21	1.03E+22	1.21E+21	1.01E+22	1.96E+22	2.22E+22	2.20E+22	2.01E+22	6.89E+21
FW gross deposition [Be/s]	1.35E+23	4.49E+22	6.39E+22	1.13E+22	9.44E+22	1.83E+23	2.07E+23	2.06E+23	1.73E+23	8.82E+22
FW gross deposition [%]	90.0	82.7	86.1	90.3	90.3	90.4	90.3	90.4	89.6	92.8
divertor gross deposition [Be/s]	1.47E+22	9.08E+21	9.99E+21	1.19E+21	9.91E+21	1.92E+22	2.18E+22	2.16E+22	1.99E+22	5.80E+21
divertor gross deposition [%]	9.8	16.7	13.5	9.5	9.5	9.5	9.5	9.5	10.3	6.1
gaps gross deposition [Be/s]	2.95E+20	2.93E+20	2.87E+20	2.27E+19	1.86E+20	3.60E+20	4.18E+20	4.25E+20	1.85E+20	1.09E+21
gap gross deposition [%]	0.2	0.5	0.4	0.2	0.2	0.2	0.2	0.2	0.1	1.1

Table 1: Summary of the surface-integrated Be erosion and deposition results of the parametric studies in comparison with the reference case.

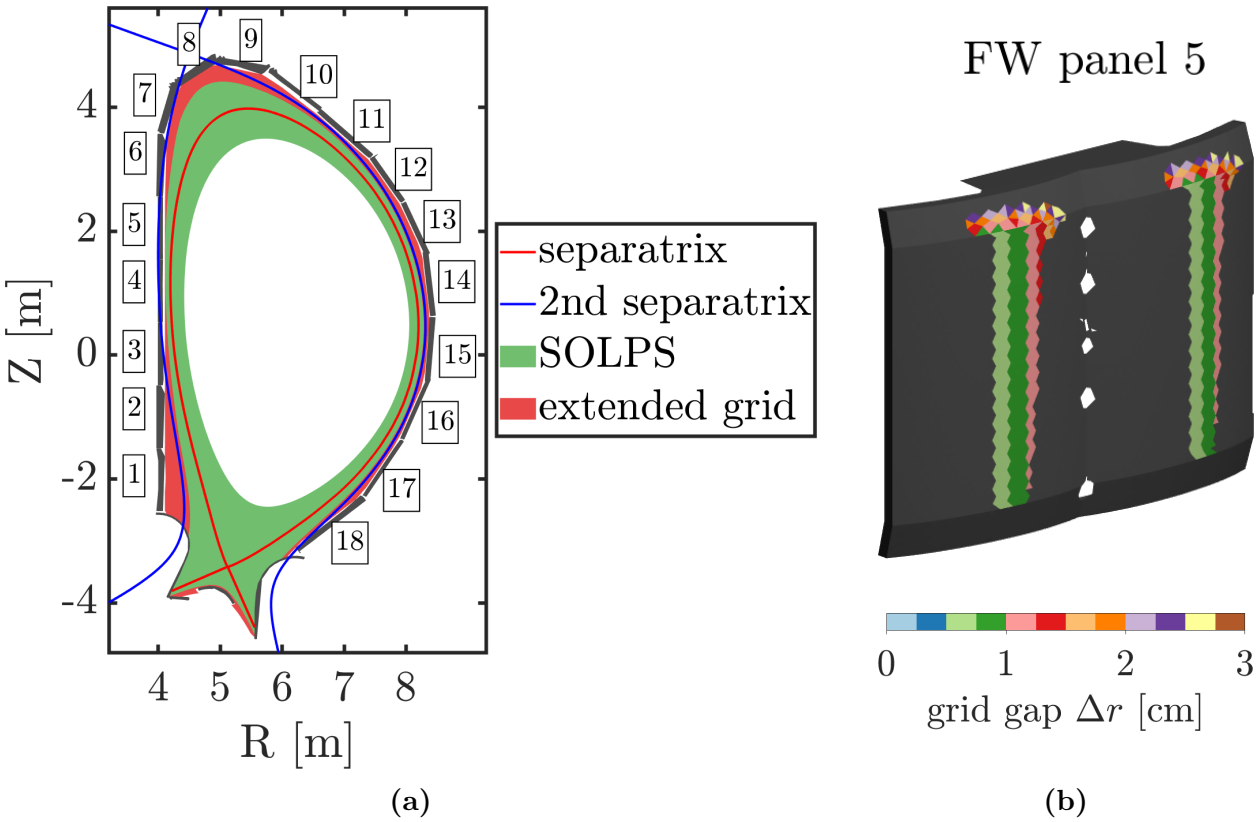

Figure 1: (a) Poloidal view of the simulated ITER geometry. The black patches numbered 1-18 indicate the individual FW panels. The colored regions indicate the SOLPS grid and the "extended grid" of the OEDGE solution. (b) Zoomed in 3D view of panel 5, with a color map indicating the distance of plasma-wetted surfaces from the OEDGE grid boundary. Grey areas are indicating magnetically shadowed areas.

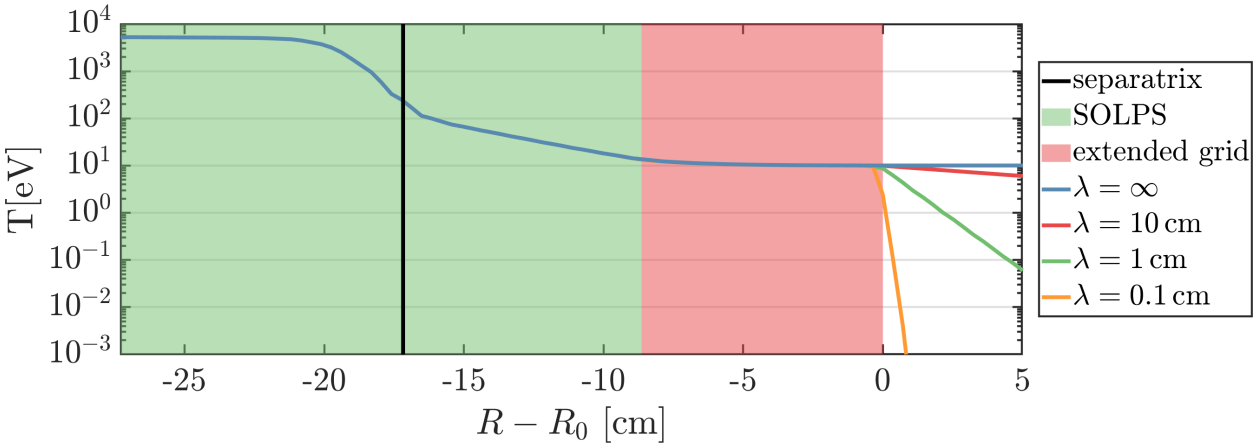

Figure 2: Outer midplane (OMP) profiles of the electron temperature. R_0 is the OEDGE outer grid boundary at the OMP. The reference case with a constant extrapolation ($\lambda = \infty$) is compared to exponentially decaying profiles obtained with a finite λ.

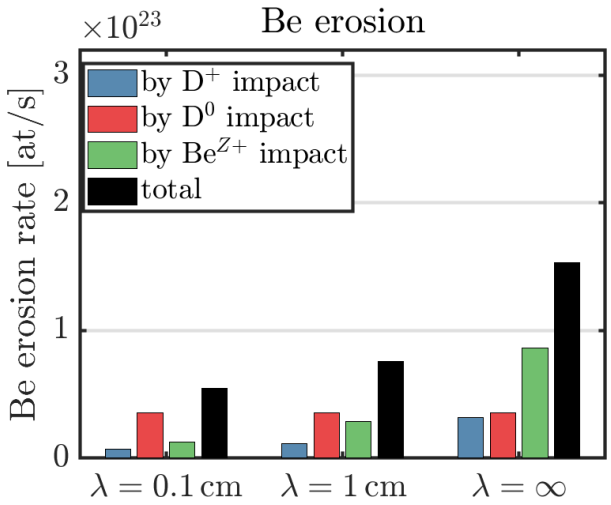

Figure 3: Be erosion rate (integrated over the FW), obtained using different decay lengths. For each case, the contributions to erosion by different impacting species (D^+, D^0 and Be^{Z+}) are shown, as well as their sum.

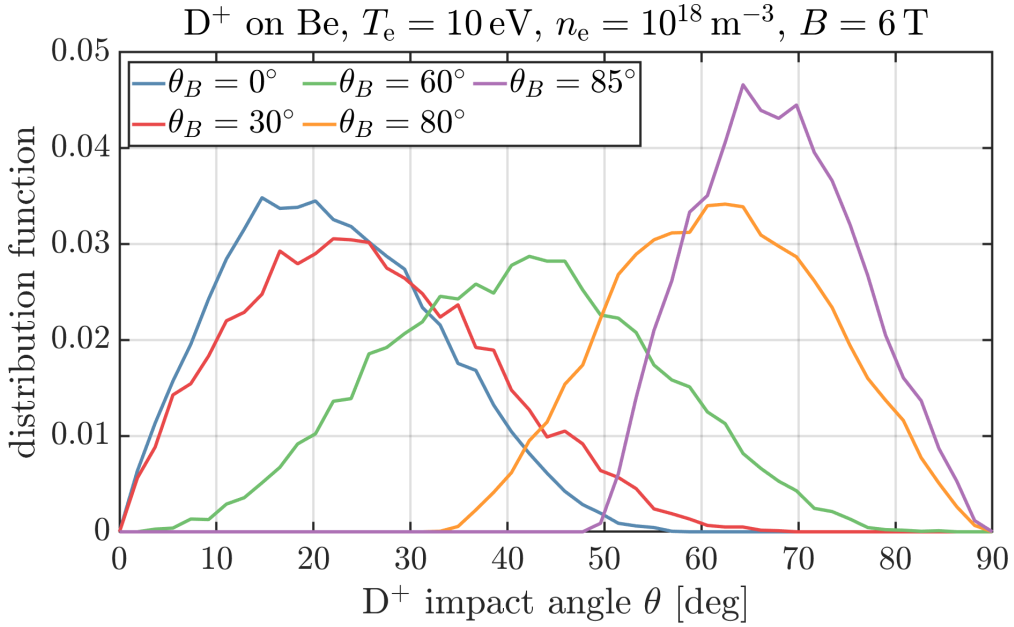

Figure 4: Distributions of the impact angle θ for D^+ ions at different magnetic inclination angles θ_B, obtained using the sheath tracing module in ERO2.0.

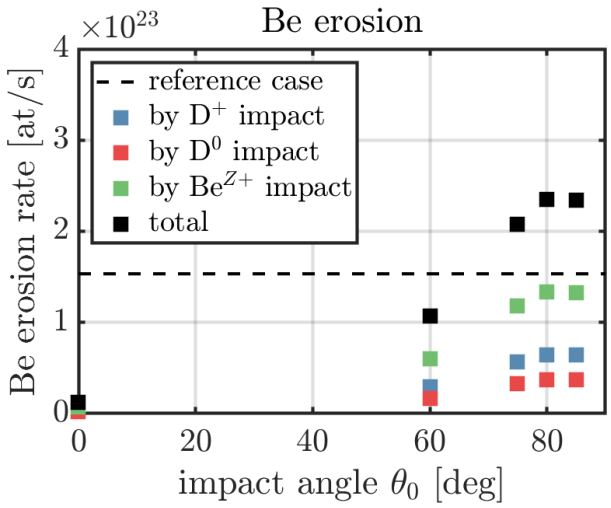

Figure 5: Be erosion rate (integrated over the FW), obtained using different constant D^+ and D^0 impact angles θ_0.

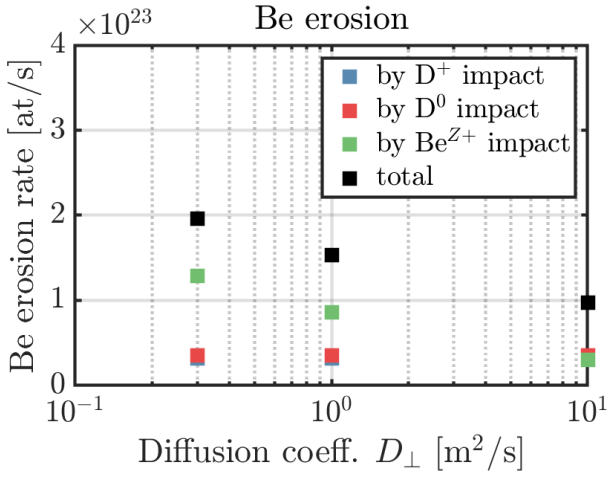

Figure 6: Be erosion rate (integrated over the FW), obtained using different constant diffusion coefficients $D_\perp$.

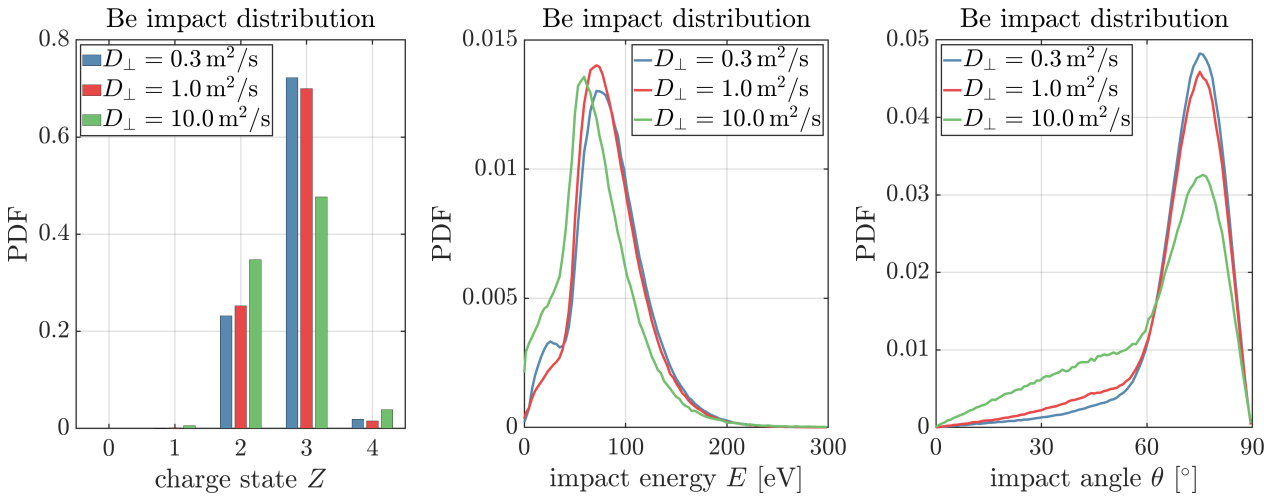

Figure 7: Distributions of impacting Be, accumulated over the entire FW, for different values of $D_\perp$.